Current Biology 16, 1719–1725, September 5, 2006 ©2006 Elsevier Ltd All rights reserved DOI 10.1016/j.cub.2006.07.020

Report

Rab35 Regulates an Endocytic Recycling Pathway Essential for the Terminal Steps of Cytokinesis

Ilektra Kouranti,[1] Martin Sachse,[1,2] Nassim Arouche,[1] Bruno Goud,[1] and Arnaud Echard[1,*]
[1] Laboratoire Mécanismes moléculaires du transport intracellulaire
Institut Curie
Centre National de la Recherche Scientifique UMR144
26 rue d'Ulm
75248 Paris cedex 05
France

Summary

Cytokinesis is the final step of cell division and leads to the physical separation of the daughter cells. After the ingression of a cleavage membrane furrow that pinches the mother cell, future daughter cells spend much of the cytokinesis phase connected by an intercellular bridge. Rab proteins are major regulators of intracellular transport in eukaryotes [1], and here, we report an essential role for human Rab35 in both the stability of the bridge and its final abscission. We find that Rab35, whose function in membrane traffic was unknown, is localized to the plasma membrane and endocytic compartments and controls a fast endocytic recycling pathway. Consistent with a key requirement for Rab35-regulated recycling during cell division, inhibition of Rab35 function leads to the accumulation of endocytic markers on numerous cytoplasmic vacuoles in cells that failed cytokinesis. Moreover, Rab35 is involved in the intercellular bridge localization of two molecules essential for the postfurrowing steps of cytokinesis: the phosphatidylinositol 4,5-bis phosphate (PIP2) lipid [2–4] and the septin SEPT2 [5]. We propose that the Rab35-regulated pathway plays an essential role during the terminal steps of cytokinesis by controlling septin and PIP2 subcellular distribution during cell division.

Results and Discussion

Recent genome-wide RNAi-based screens highlighted the fact that intracellular transport is essential for animal cytokinesis [6–8], with both the secretory and the endocytic pathways being implicated in the late phases of cytokinesis [9–17]. Among the key regulators of membrane trafficking in eukaryotes, Rab GTPases represent a large family of proteins that define particular routes within the secretory and endocytic pathways by controlling several transport steps such as vesicle formation, motility, docking, and fusion [1]. In particular, Rab11 is required for cytokinesis in a variety of systems [9, 18], and it has been the only Rab implicated so far in this process in mammalian cells [12]. To determine whether other Rabs are required for cytokinesis, we used RNA interference (RNAi)-mediated gene inactivation to test which ones are essential for this process. The Rab family in mammals is large (>60 members), and the presence of multiple isoforms that could be functionally redundant complicates such an analysis [19]. Because many cytokinesis genes are conserved among metazoans [17], we decided to first identify which Rabs are essential for cytokinesis in *Drosophila*, which encodes fewer Rab proteins and in which RNAi is efficient. We thus systematically down-regulated each of the 29 *Rab* genes in *Drosophila* S2-cultured cells and monitored the appearance of binucleated cells as an indicator of cytokinesis failure (Figure 1A). An increase in binucleated cells was observed after Rab5 and Rab11 depletion. This finding is consistent with previous work showing that Rab5 and Rab11 proteins are implicated in *Drosophila* cellularization, an event that is related to cytokinesis [18]. However, inactivation of *Drosophila* Rab35 led to the strongest increase in binucleated cells, with 20% cells after a 6 day RNAi treatment (Figure 1A); this result indicates that this Rab is essential for cytokinesis.

Rab35 is phylogenetically conserved in metazoans, with a single orthologous gene being expressed in humans [19]. To investigate whether human Rab35 is involved in cytokinesis, we monitored division in HeLa cells after the inhibition of Rab35 function either by overexpression of a dominant-negative mutant (Rab35 S22N) or after RNAi-mediated depletion. We first analyzed the accumulation of multinucleated cells on fixed samples after transfection of the Rab35 S22N mutant for 3 days and observed a 13.5-fold increase of binucleated cells above background levels (21.9% ± 1.2% versus 1.6% ± 0.2% in controls, n = 3, >500 cells per experiment, t test $p < 0.001$). This phenotype was consistent with a specific inhibition of Rab35 function because the number of binucleated cells also increased by 3.5-fold (4.1% ± 0.4% versus 1.1% ± 0.2% in controls, n = 3, >500 cells per experiment, t test $p = 0.004$) after reduction of Rab35 protein levels by a 5 day RNAi treatment. Importantly, inhibition of Rab35 function by either RNAi or Rab35 S22N overexpression did not affect the levels of endogenous Rab5 and Rab11, suggesting that impairing Rab35 function has a direct effect on cytokinesis (see Figure S1 in the Supplemental Data available with this article online). We conclude from these observations that Rab35, as in *Drosophila* cells, is essential for cytokinesis in human cells.

To determine at which stage of cytokinesis Rab35 is required, we analyzed by time-lapse microscopy the progression through mitosis after inhibition of Rab35 function. Videomicroscopy analysis revealed that mitotic cell rounding, anaphase progression, cell elongation, and furrow ingression appeared normal after Rab35 S22N overexpression (Figure S2) or reduction of Rab35 levels by RNAi (Figures 1B and 1C). In both cases, binucleated cells arose from a destabilization of the

*Correspondence: arnaud.echard@curie.fr
[2] Present address: Plate-forme de Microscopie Electronique, Institut Pasteur, 28 rue du Dr Roux, 75724 Paris Cedex 15, France.

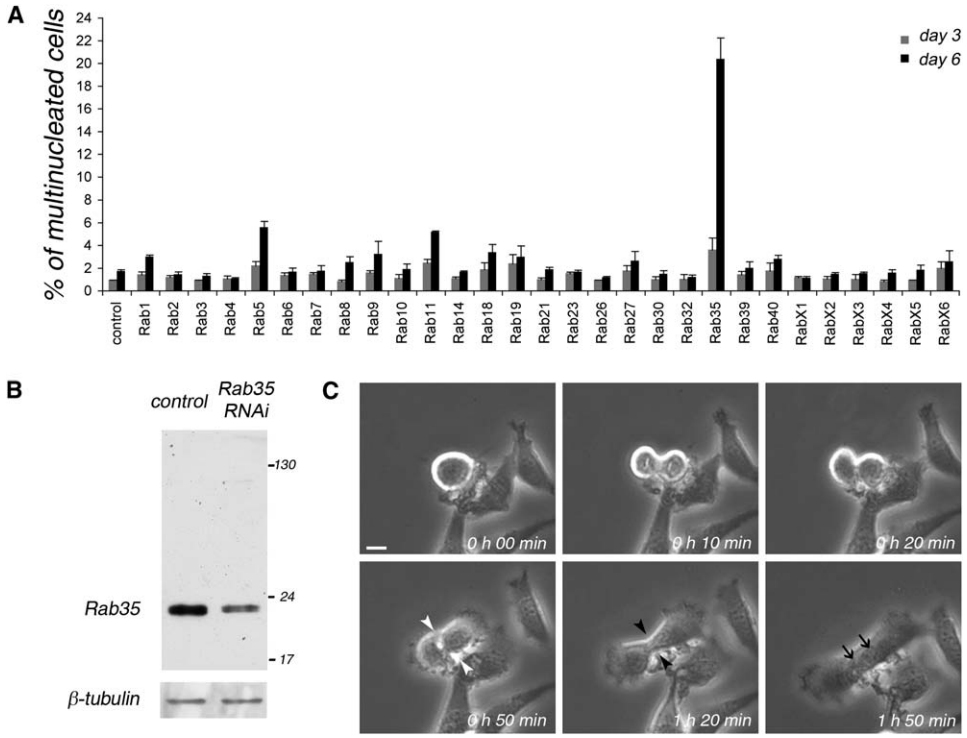

Figure 1. Rab35 Is Required for Postfurrowing Steps of Cytokinesis

(A) *Drosophila* S2 cells were treated for 3 days or 6 days with dsRNA that interfered with each *Rab* gene encoded by the *Drosophila* genome. The number of multinucleated cells in each condition was counted (mean ± SEM, n = 3, >500 cells per condition) and represented ~1% to 2% in control experiments. For comparison, inactivation of the cytokinesis genes *pebble* and *diaphanous* led to 37% and 4% binucleated cells at day 3 and 63% and 23% at day 6, respectively.

(B) After control or Rab35 RNAi, extracts from HeLa cells were analyzed by Western blot with Rab35 antibodies to monitor protein knockdown efficiency after a 5-day treatment. β-tubulin levels were used as a loading control.

(C) Selected phase contrast time-lapse videomicroscopy frames from HeLa cells after Rab35 RNAi. This cell entered mitosis 100 hr posttransfection, progressed normally through mitosis, and formed an intercellular bridge (marked by white arrowheads) that destabilized (marked by black arrowheads), giving rise to a binucleated cell (marked by black arrows). Cytokinesis failed in 27/911 (3%) dividing cells after Rab35 knockdown. In comparison, it failed in 6/663 (0.9%) control cells. These results are in agreement with fixed cell analysis (see text). The scale bar represents 10 μm.

intercellular bridge (Figures S2 and 1C), indicating that Rab35 is required for stabilizing the cytokinesis bridge connecting daughter cells after furrow ingression. In addition, the time required for abscission was strongly increased in the cells that did not become binucleated after Rab35 S22N overexpression or after Rab35 knockdown by RNAi (Figure S3). We conclude that both dominant-negative and RNAi-mediated depletion approaches demonstrate that Rab35 is required in human cells for the postfurrowing terminal steps of cytokinesis, namely for bridge stability and abscission. Because RNAi-mediated Rab35 depletion was not complete even after prolonged treatment (Figure 1B) and led to a similar but less penetrant cytokinesis phenotype, we used the dominant-negative approach as a tool to potently inhibit Rab35 function in the experiments described hereafter in this work.

To get insight into Rab35 function during the postfurrowing steps of cytokinesis, we next investigated its localization and its role in membrane trafficking. Two rabbit antisera were raised against recombinant human Rab35. They specifically recognized endogenous Rab35 protein in HeLa cell extracts, as demonstrated by the reduction of the signal after RNAi (Figure 1B and data not shown). After fractionation of postnuclear supernatant, endogenous Rab35 was found to be predominantly (~70%) associated with cell membranes (data not shown). Immunofluorescence and immunoelectron microscopy (EM) experiments revealed that endogenous Rab35 was associated with the plasma membrane and internal structures (Figures 2A and 2B). To further investigate Rab35 localization to the plasma membrane, we transfected cells with PLC-δ-PH-GFP, a probe for the phosphatidylinositol 4,5-bis phosphate (PIP2) [20]. Most Rab35 was detected in PIP2-positive domains (Figure 2A, arrowheads), although it could also be found in areas devoid of PIP2 (Figure 2A, arrows). Quantification of EM sections indicated that about 30% of the endogenous Rab35 was associated with the plasma membrane, where it concentrated at membrane extensions and on clathrin-coated pits (Figure 2B_i; see also Figure S4). Double-labeling experiments with internalized transferrin revealed that Rab35 localized to endocytic clathrin-coated vesicles (Figures 2B_i–2B_{ii}) and that ~10% of endogenous Rab35 was present on sorting endosomes and endosomal tubules (Figure 2B_{iv}; see also Figure S4). A small pool of endogenous Rab35 was also found on vesicles that were

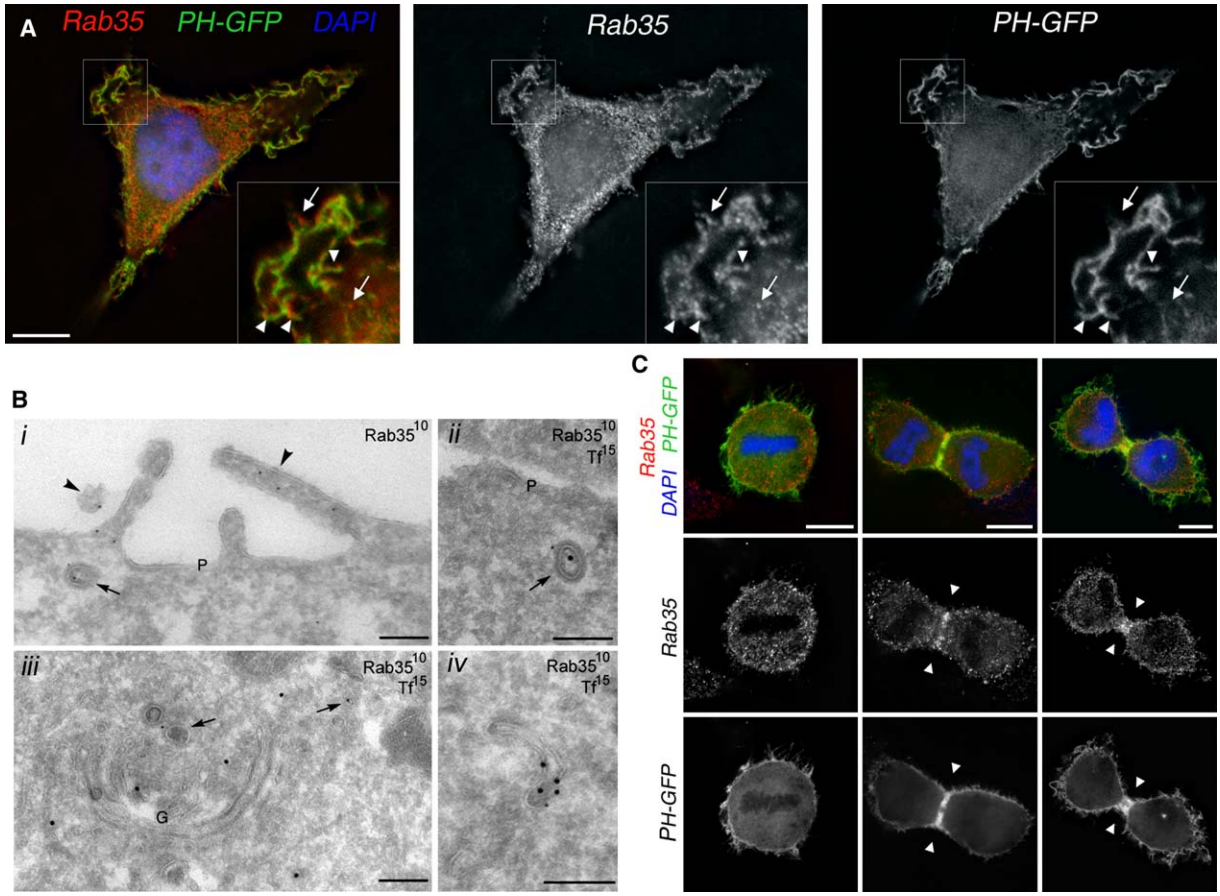

Figure 2. Rab35 Is Localized to the Plasma Membrane and to Endocytic Compartments and Colocalizes with PIP2 to the Intercellular Bridge during Cytokinesis

(A) HeLa cells were transfected with a PLC-δ-PH-GFP (a PIP2 probe)-encoding plasmid for 24 hr and processed for immunofluorescence (GFP is in green, endogenous Rab35 is in red, and DAPI is in blue). The left panel displays overlay channels of an entire cell and a zoom region of the plasma membrane. Middle and right panels correspond to single staining in gray levels as indicated. Rab35 largely colocalized with PIP2 at the plasma membrane (arrowheads) but was also found in structures lacking PIP2 (arrows). Scale bars represent 10 μm.

(B) Immuno-EM localization of endogenous Rab35 (10 nm gold particles) (i) or Rab35 (10 nm) and biotin (15 nm) (ii–iv) after a 30 min uptake of biotinylated transferrin (Tf). In (i), P indicates plasma membrane, arrowheads mark membrane protrusions, and the arrow marks a clathrin-coated vesicle. In (ii), the arrow marks a clathrin-coated vesicle. In (iii), the arrows mark the peri Golgi (G) area. (iv) shows endocytic recycling transport intermediates. Scale bars represent 200 nm. See Figure S4 for quantification.

(C) PLC-δ-PH-GFP (green) and Rab35 (red) localizations in mitotic HeLa cells processed as described in (A). Overlay stainings of successive stages of mitosis (metaphase, anaphase, and telophase) are displayed in the upper panels, and single stainings are displayed in gray levels. Rab35 and PIP2 largely colocalize at the ingressing furrow and at the midbody region during late cytokinesis (arrowheads). Scale bars represent 10 μm. In (A) and (C), each image corresponds to a single plane.

transferrin-negative and located in close vicinity to the Golgi apparatus, but not within the Golgi stacks (Figure 2B$_{iii}$; see also Figure S4). A Myc-tagged version of Rab35 was found at the same locations as endogenous Rab35 at the immunofluorescence and EM resolutions (Figure S5). As in interphase cells, endogenous Rab35 (Figure 2C) or Myc-tagged Rab35 (Figure S5) was associated with the plasma membrane during mitosis and was present at the ingressing furrow during early cytokinesis phases as well as at the intercellular bridge later during cytokinesis. Interestingly, Rab35 colocalized in these structures with PIP2, which was recently shown to be enriched at the intercellular bridge during cytokinesis [2, 4] (Figure 2C, arrowheads).

The localization of Rab35 prompted us to test whether it controls trafficking between the plasma membrane and endocytic compartments. We first investigated the possible role of Rab35 during initial steps of endocytosis and found that cells expressing Rab35 S22N internalized surface-bound transferrin with identical initial rates as those of control cells (Figure 3A, time points <10 min). However, internalized transferrin recycled back to the extracellular medium with slower kinetics in cells expressing Rab35 S22N (Figure 3A, time points >15 min), suggesting that Rab35 regulates a recycling step. To directly demonstrate that Rab35 was involved in a recycling pathway, we loaded cells with fluorescently labeled transferrin for 30 min and measured the kinetics of chase after transfer into a medium containing unlabeled transferrin. Half of the internalized transferrin recycled back to the plasma membrane within 26 min ± 2 min in cells expressing the Rab35 S22N mutant, as compared to 16 min ± 2 min in control cells (Figure 3B), indicating that recycling was perturbed. At least two

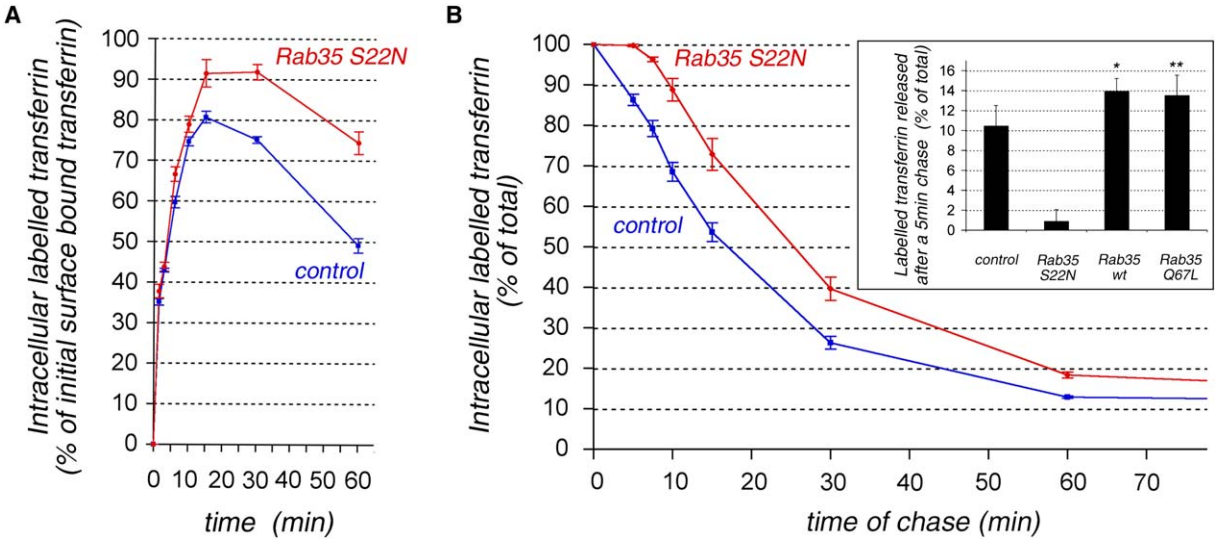

Figure 3. Rab35 Controls a Fast Recycling Transport Step from Endosomal Compartments to the Plasma Membrane

HeLa cells were transfected with either control (blue curve) or dominant-negative Rab35 S22N (red curve)-expressing plasmids for 72 hr.

(A) Internalization and recycling of surface bound transferrin; fluorescently labeled transferrin was bound to the cell surface for 45 min at 4°C. Nonspecific binding was washed out, and cells were allowed to internalize and recycle transferrin for different times (*x* axis) at 37°C. The intracellular, labeled transferrin was quantified, and results were expressed as the fraction of initial surface bound transferrin (*y* axis) (mean ± SEM, n = 3, >2000 cells were analyzed by cytometry for each time point). Note that the number of TfR at the surface was reduced in Rab35 S22N-expressing cells compared to control cells but that initial rates of internalization were identical (see text).

(B) Transfected cells were loaded with fluorescently labeled transferrin by continuous uptake at 37°C for 30 min. TfR recycling to the cell surface was measured by quantification of intracellular, labeled transferrin (y-axis) that remained after different chase times at 37°C (x-axis) into a medium containing unlabeled transferrin. The results are expressed as the intracellular fraction of the loaded transferrin (mean ± SEM, n = 3, 2000–9000 cells were analyzed by cytometry for each time point). (B inset) Fast recycling after a 5 min chase was measured as described above in HeLa cells transfected with control, Rab35 S22N-, Rab35 wild-type-, or Rab35 Q67L-encoding plasmids 72 hr posttransfection. The results are expressed as the fraction of loaded transferrin that was released from cells for each condition (mean ± SEM, n = 4, 2000–9000 cells were analyzed per experiment). Fast recycling is strongly inhibited by the Rab35 S22N mutant, whereas overexpression of wild-type or GTP-locked Rab35 Q67L mutant significantly increases fast recycling; paired t test values were p = 0.02 and p = 0.001 for * and ** comparisons with control, respectively.

recycling pathways have been described in mammalian cells: a direct or fast recycling pathway that operates from peripheral endocytic compartments and a slow recycling pathway that recycles molecules back to the plasma membrane from deeper compartments with slower kinetics. Recycling rates for chase times of more than 15 min did not appear to be significantly affected in cells overexpressing Rab35 S22N, suggesting that slow recycling was not perturbed (Figure 3B). Strikingly, the fast recycling, as measured after a 5 min chase, appeared strongly reduced in cells expressing Rab35 S22N (Figure 3B, inset). Conversely, overexpression of wild-type or GTPase-deficient (GTP-locked) Rab35 Q67L mutant significantly increased fast recycling (paired t test with p = 0.02 and p = 0.001, respectively, n = 4, >2000 cells per experiment) (Figure 3B, inset), suggesting that Rab35 is an essential rate-limiting regulator of fast recycling. The involvement of Rab35 in a recycling transport step to the plasma membrane was further confirmed by the observation that the amount of transferrin receptor (TfR) at the cell surface was reduced in cells overexpressing Rab35 S22N (Figure S6). Quantification by FACS cytometry indeed revealed a 2-fold reduction in the number of surface binding sites for transferrin (52% ± 3% of control, mean ± SEM, n = 6, >2000 cells analyzed per experiment), which is consistent with a defective recycling of receptors back to the PM in Rab35 S22N-expressing cells. We conclude from the above experiments that Rab35 is not involved in an internalization transport step but controls a fast recycling pathway back to the PM.

To investigate whether defective recycling could be the cause of the cytokinesis defects in Rab35 S22N-expressing cells, we analyzed TfR recycling during early and late phases of cytokinesis. Given the brief time frame of furrow ingression in anaphase and bridge formation in telophase, it was technically not feasible to directly measure transferrin recycling during these particular phases of the cell cycle by cytometry, as we did in interphase cells. However, amounts of plasma-membrane-associated TfR were reduced during furrow ingression (Figures 4A and 4B) and when intercellular bridges still connected daughter cells (Figures 4C and 4D) after Rab35 S22N expression. Semi-quantitative analysis of immunofluorescence images revealed a mean 2-fold reduction of surface TfR levels during cytokinesis in Rab35 S22N-expressing cells; this reduction is in good agreement with values obtained in interphase cells. This result indicates that, as in interphase cells, recycling to the cell surface is also impaired during cytokinesis upon Rab35 inhibition. Consistent with a defective recycling, the TfR accumulated in numerous intracellular vacuoles that formed in approximately 30% of posttelophase cells that failed cytokinesis after Rab35 S22N overexpression (Figure 4G); such localization was never seen in control cells (Figure 4E). This abnormal

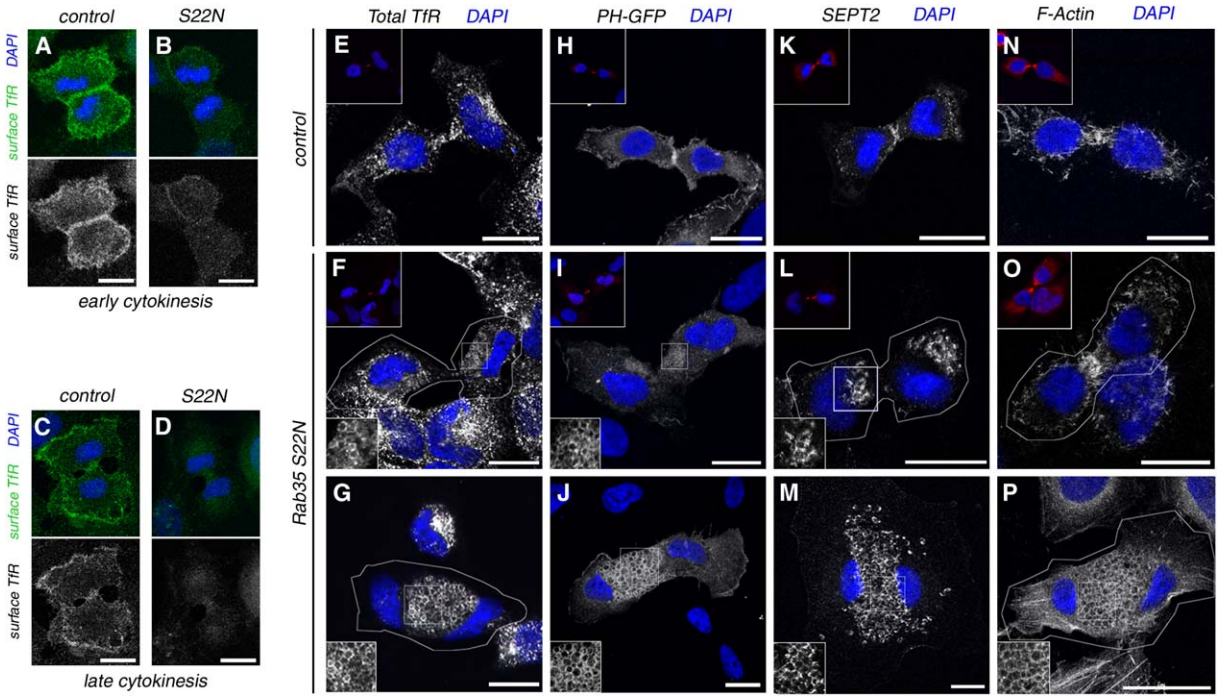

Figure 4. Rab35 Functions in a Recycling Step during Cytokinesis That Controls PIP2 and SEPT2 Localization to the Intercellular Bridge

(A–D) HeLa cells were transfected with control (A and C) or Rab35 S22N (B and D)-encoding plasmids for 72 hr and processed for immunofluorescence. Cells during cytokinesis furrow ingression (early cytokinesis shown in [A] and [B]) or connected by an intercellular bridge (late cytokinesis shown in [C] and [D]) were stained in green for TfR without permeabilization (surface TfR labeling). TfR recycling to the plasma membrane during all phases of cytokinesis was reduced in mutant cells compared to controls.

(E–P) HeLa cells were transfected with control (E, H, K, and N) or Rab35 S22N mutant-encoding plasmids (F–G, I–J, L–M, and O–P) for 72 hr and processed for immunofluorescence. Transfected cells were outlined in white where it was necessary. In (H)–(J), the PLC-δ-PH-GFP-encoding plasmid was cotransfected. Cells were stained for TfR (total TfR staining after permeabilization) in (E)–(G), for GFP in (H)–(J), for SEPT2 in (K)–(M), and for F-actin (phalloidin) in (N)–(P). Corresponding stainings are displayed in gray levels and have been overlaid with DAPI in blue. Cells in the first two rows are in cytokinesis and are still connected by an intercellular bridge, as shown in upper-left insets (Rabkinesin-6 stainings in [E]–[F] and [H]–[I] or tubulin stainings in [K]–[L], and [N]–[O] in red). Cells in (G), (J), (M), and (P) were fixed after cytokinesis failed and contained two nuclei. In contrast to punctuated structures observed in control cells (E), the TfR accumulates on numerous intracellular vacuoles in the Rab35 S22N-expressing cells (F–G). PIP2 and the septin SEPT2 are restricted to the plasma membrane and are enriched at the intercellular bridge during cytokinesis in control cells (H and K) but not in Rab35 S22N-expressing cells (I and L). PIP2 and SEPT2 instead accumulated on intracellular vacuoles (I–J and L–M). Mislocalization of TfR, PIP2, and SEPT2 markers on intracellular vacuoles is displayed at a higher magnification in bottom-left zoom regions. In contrast to PIP2 and SEPT2, F-actin was normally enriched at the intercellular bridge in Rab35 S22N-expressing cells (O), as observed in controls (N). In addition, F-actin was enriched on large intracellular vacuoles after cytokinesis failed (P; see text). Each image corresponds to a single confocal plane. Scale bars represent 20 μm.

localization was observed not only after cytokinesis failed (Figure 4G) but also when the daughter cells were still connected before the bridge destabilized (Figure 4F). The reduction of endogenous Rab35 by RNAi was not complete (Figure 1B), which likely explains why no intracellular vacuoles were observed in Rab35-depleted cells. However, the number of Rab35 S22N-overexpressing cells that formed vacuoles increased by 58% ± 5% after endogenous Rab35 knockdown (>300 cells per experiment, n = 5, t test p = 0.005, see the Supplemental Experimental Procedures for details). In addition, we never observed the formation of vacuoles in cells that overexpressed dominant-negative mutants of two Rab proteins involved in endocytic recycling (Rab4 and Rab11) and cytokinesis (Rab11). These results are consistent with a specific inhibition of Rab35 recycling function by Rab35 S22N.

The stability of the intercellular bridge and the abscission step of cytokinesis involve targeted membrane addition close to the midbody region and the establishment of particular protein and lipid domains within the bridge [15, 16]. In particular, it has been shown that production and turnover of PIP2 are required for cytokinesis in different organisms [2–4, 21–23] and that PIP2 localization at the bridge is essential for bridge stability and cytokinesis completion in mammalian cells [2]. As recently reported [2, 4], we found that PIP2 is associated to the plasma membrane and greatly enriched at the intercellular bridge during late stages of cytokinesis in control cells (Figure 4H). Interestingly, quantifications on fixed samples revealed that 55% of the intercellular bridges connecting daughter cells expressing Rab35 S22N (n = 75) lacked any PIP2 enrichment (Figure 4I); in comparison, 24% of control bridges (n = 75) lacked PIP2 enrichment at the same stage of cytokinesis (Figure 4H). In addition, PIP2 was found to mislocalize into the intracellular vacuoles positive for TfR in Rab35 S22N-overexpressing cells when they were still connected by an intercellular bridge (Figure 4I) or when cytokinesis already failed (Figure 4J). Moreover, the

number of cells in which PIP2 was delocalized from the intercellular bridge after Rab35 S22N overexpression was increased by 27% after endogenous Rab35 knockdown by RNAi (n = 55). We thus conclude that Rab35 contributes to the proper localization and maintenance of PIP2 at the intercellular bridge during cytokinesis.

How exactly PIP2 contributes to cytokinesis is currently unknown, but it could recruit cytoskeletal proteins, such as septins, that are essential for this process. The septin SEPT2 is enriched at the furrow and at the intercellular bridge during cytokinesis [5] and is likely to bind to PIP2 via a conserved basic domain, as already shown for SEPT4/Septin H5 [24]. Because functional inactivation of SEPT2 in mammalian cells leads to cytokinesis defects similar to those observed after Rab35 inhibition (binucleated cells and abnormal abscission) [5], we thus analyzed the localization of this septin in Rab35 S22N-expressing cells. We found that, as shown for PIP2, 52% of the intercellular bridges connecting daughter cells expressing Rab35 S22N (n = 33) displayed no SEPT2 enrichment (Figure 4L); in comparison, only 15% of control bridges (n = 33) displayed no SEPT2 enrichment at the same stage of cytokinesis (Figure 4K). Instead, SEPT2 was found on intracellular vacuoles when cells were still connected (Figure 4L) or after cytokinesis failed (Figure 4M). By contrast, anillin (data not shown) and F-actin (Figures 4N–4O) were properly localized at the ingressing furrow and at the intercellular bridge after Rab35 S22N overexpression. We noticed that F-actin often localized on the very large intracellular vacuoles that grew after cytokinesis failed (Figure 4P). A likely hypothesis is that PIP2 progressively induces actin polymerization at the surface of these vacuoles. Moreover, anillin was exceptionally found on those very large vacuoles (data not shown). Because SEPT2 and PIP2 localization at the bridge are required for its stability and cytokinesis completion in mammalian cells [2, 5], we propose that the Rab35-regulated pathway has an essential role for cytokinesis in controlling PIP2 and SEPT2 localization during the late stages of cytokinesis.

In conclusion, we report that Rab35 is a regulator of an endocytic recycling pathway that is essential for bridge stability and abscission. Such a requirement in cytokinesis is likely to be phylogenetically conserved in metazoans because Rab35 is essential for this process in both *Drosophila* and human cells. Rab11 is another Rab essential for cytokinesis in mammals and is required after furrow ingression [12]. Interestingly, Rab11 and Rab35 are localized to different subcellular compartments and control distinct endocytic recycling pathways ([1] and this study), suggesting that multiple endocytic routes are individually essential for cytokinesis. Finally, our work reveals that the Rab35-regulated pathway contributes to the SEPT2 and PIP2 lipid localization at the intercellular bridge during late cytokinesis and helps us to understand how lipid domains that are essential for the terminal steps of cytokinesis are established.

Supplemental Data

Supplemental data include Supplemental Experimental Procedures and six figures and can be found at http://www.current-biology.com/cgi/content/full/16/17/1719/DC1/.

Acknowledgments

We are grateful to T. Balla for plasmids; to Dr. Trimble for antibodies; to J. Young, S. Delaire, S. Miserey-Lenkei, M. Morgan, and Y. Bellaiche for critical comments on the manuscript and discussions; to the Staff Imagerie and S. Miserey-Lenkei for assistance in image acquisition; and to C. Théry for cytometry analysis training. I.K. was supported by a fellowship from the Ministère de l'Education Nationale de la Recherche et de la Technologie, and M.S. by the Fondation pour la Recherche Médicale (FRM grant ACE20030926192). The research was supported by the Centre National de la Recherche Scientifique (ACI), the Institut CURIE (Programmes incitatifs et coopératifs "Paramètres épigénétiques" and Programmes incitatifs et coopératifs "Physique du vivant") and the Association pour la Recherche sur le Cancer (ARC grant 3269).

Received: April 5, 2006
Revised: July 5, 2006
Accepted: July 6, 2006
Published: September 5, 2006

References

1. Zerial, M., and McBride, H. (2001). Rab proteins as membrane organizers. Nat. Rev. Mol. Cell Biol. *2*, 107–117.
2. Emoto, K., Inadome, H., Kanaho, Y., Narumiya, S., and Umeda, M. (2005). Local change in phospholipid composition at the cleavage furrow is essential for completion of cytokinesis. J. Biol. Chem. *280*, 37901–37907.
3. Wong, R., Hadjiyanni, I., Wei, H.C., Polevoy, G., McBride, R., Sem, K.P., and Brill, J.A. (2005). PIP2 hydrolysis and calcium release are required for cytokinesis in *Drosophila* spermatocytes. Curr. Biol. *15*, 1401–1406.
4. Field, S.J., Madson, N., Kerr, M.L., Galbraith, K.A., Kennedy, C.E., Tahiliani, M., Wilkins, A., and Cantley, L.C. (2005). PtdIns(4,5)P2 functions at the cleavage furrow during cytokinesis. Curr. Biol. *15*, 1407–1412.
5. Kinoshita, M., Kumar, S., Mizoguchi, A., Ide, C., Kinoshita, A., Haraguchi, T., Hiraoka, Y., and Noda, M. (1997). Nedd5, a mammalian septin, is a novel cytoskeletal component interacting with actin-based structures. Genes Dev. *11*, 1535–1547.
6. Skop, A.R., Liu, H., Yates, J., 3rd, Meyer, B.J., and Heald, R. (2004). Dissection of the mammalian midbody proteome reveals conserved cytokinesis mechanisms. Science *305*, 61–66.
7. Echard, A., Hickson, G.R., Foley, E., and O'Farrell, P.H. (2004). Terminal cytokinesis events uncovered after an RNAi screen. Curr. Biol. *14*, 1685–1693.
8. Eggert, U.S., Kiger, A.A., Richter, C., Perlman, Z.E., Perrimon, N., Mitchison, T.J., and Field, C.M. (2004). Parallel chemical genetic and genome-wide RNAi screens identify cytokinesis inhibitors and targets. PLoS Biol. *2*, e379.
9. Skop, A.R., Bergmann, D., Mohler, W.A., and White, J.G. (2001). Completion of cytokinesis in *C. elegans* requires a brefeldin A-sensitive membrane accumulation at the cleavage furrow apex. Curr. Biol. *11*, 735–746.
10. Gromley, A., Yeaman, C., Rosa, J., Redick, S., Chen, C.T., Mirabelle, S., Guha, M., Sillibourne, J., and Doxsey, S.J. (2005). Centriolin anchoring of exocyst and SNARE complexes at the midbody is required for secretory-vesicle-mediated abscission. Cell *123*, 75–87.
11. Schweitzer, J.K., and D'Souza-Schorey, C. (2002). Localization and activation of the ARF6 GTPase during cleavage furrow ingression and cytokinesis. J. Biol. Chem. *277*, 27210–27216.
12. Wilson, G.M., Fielding, A.B., Simon, G.C., Yu, X., Andrews, P.D., Hames, R.S., Frey, A.M., Peden, A.A., Gould, G.W., and Prekeris, R. (2005). The FIP3-Rab11 protein complex regulates recycling endosome targeting to the cleavage furrow during late cytokinesis. Mol. Biol. Cell *16*, 849–860.
13. Fielding, A.B., Schonteich, E., Matheson, J., Wilson, G., Yu, X., Hickson, G.R., Srivastava, S., Baldwin, S.A., Prekeris, R., and Gould, G.W. (2005). Rab11–FIP3 and FIP4 interact with Arf6 and the exocyst to control membrane traffic in cytokinesis. EMBO J. *24*, 3389–3399.

14. Schweitzer, J.K., Burke, E.E., Goodson, H.V., and D'Souza-Schorey, C. (2005). Endocytosis resumes during late mitosis and is required for cytokinesis. J. Biol. Chem. *280*, 41628–41635.
15. Schweitzer, J.K., and D'Souza-Schorey, C. (2004). Finishing the job: Cytoskeletal and membrane events bring cytokinesis to an end. Exp. Cell Res. *295*, 1–8.
16. Albertson, R., Riggs, B., and Sullivan, W. (2005). Membrane traffic: A driving force in cytokinesis. Trends Cell Biol. *15*, 92–101.
17. Glotzer, M. (2005). The molecular requirements for cytokinesis. Science *307*, 1735–1739.
18. Pelissier, A., Chauvin, J.P., and Lecuit, T. (2003). Trafficking through Rab11 endosomes is required for cellularization during *Drosophila* embryogenesis. Curr. Biol. *13*, 1848–1857.
19. Pereira-Leal, J.B., and Seabra, M.C. (2001). Evolution of the Rab family of small GTP-binding proteins. J. Mol. Biol. *313*, 889–901.
20. Varnai, P., and Balla, T. (1998). Visualization of phosphoinositides that bind pleckstrin homology domains: Calcium- and agonist-induced dynamic changes and relationship to myo-[3H]inositol-labeled phosphoinositide pools. J. Cell Biol. *143*, 501–510.
21. Saul, D., Fabian, L., Forer, A., and Brill, J.A. (2004). Continuous phosphatidylinositol metabolism is required for cleavage of crane fly spermatocytes. J. Cell Sci. *117*, 3887–3896.
22. Giansanti, M.G., Bonaccorsi, S., Kurek, R., Farkas, R.M., Dimitri, P., Fuller, M.T., and Gatti, M. (2006). The class I PITP Giotto is required for *Drosophila* cytokinesis. Curr. Biol. *16*, 195–201.
23. Janetopoulos, C., Borleis, J., Vazquez, F., Iijima, M., and Devreotes, P. (2005). Temporal and spatial regulation of phosphoinositide signaling mediates cytokinesis. Dev. Cell *8*, 467–477.
24. Zhang, J., Kong, C., Xie, H., McPherson, P.S., Grinstein, S., and Trimble, W.S. (1999). Phosphatidylinositol polyphosphate binding to the mammalian septin H5 is modulated by GTP. Curr. Biol. *9*, 1458–1467.